Electronic Supporting Information

Understanding the Effect of Solvent Vapor Annealing on Solution-Processed A-D-A Oligothiophene Bulk-Heterojunction Solar Cells: the Role of the Side Alkyl Chains

Cordula D. Wessendorf,*[a] Ana Perez-Rodriguez,[b] Jonas Hanisch,[a] Andreas P. Arndt,[c] Ibrahim Ata,[d] Gisela L. Schulz,[d] Aina Quintilla,[e] Peter Bäuerle,[d] Uli Lemmer,[c,e] Peter Wochner,[f] Erik Ahlswede[a] and Esther Barrena*[b]

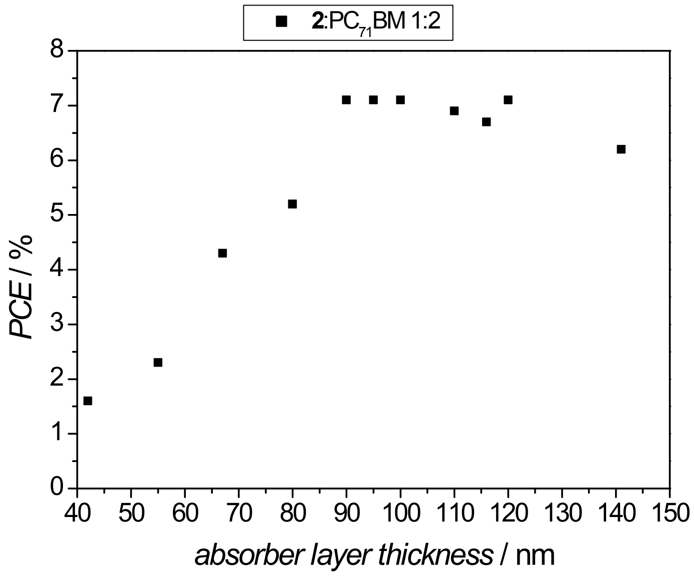

Fig. S1 **2**:$PC_{71}BM$ gives good efficiencies in a relative broad thickness range: >6.5 % PCE from 90-120 nm.

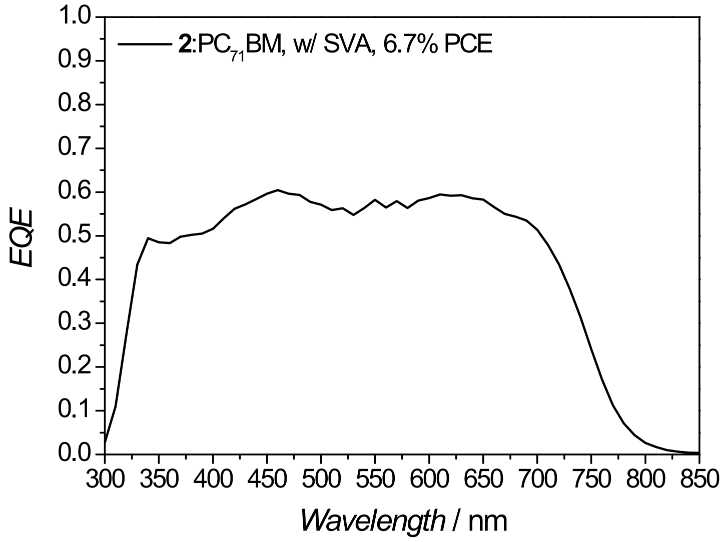

Fig. S2 External quantum efficiency spectrum of **2**:$PC_{71}BM$ solar cell after SVA.

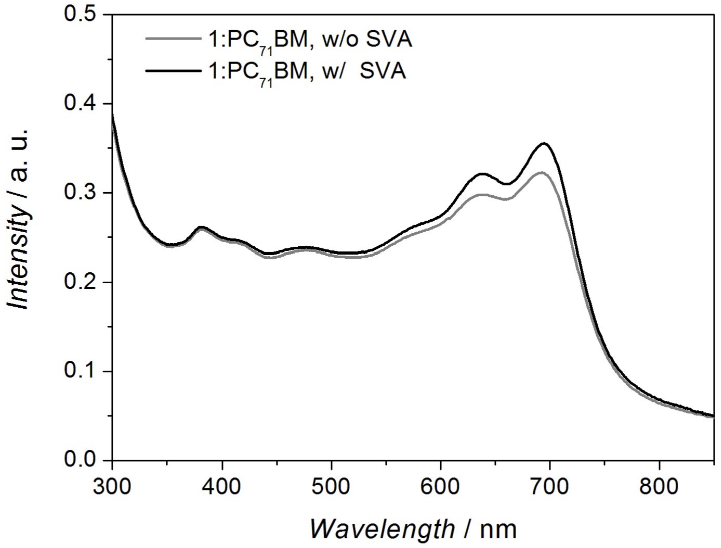

Fig. S3 Absorption spectra of **1**:$PC_{71}BM$ films without (grey line) and with (black line) SVA.

Without SVA: λ_{max} = 381, 410 (shoulder), 478, 580 (shoulder), 638, 693 nm.
With SVA: λ_{max} = 381, 410, 477, 581 (shoulder), 640, 694 nm.

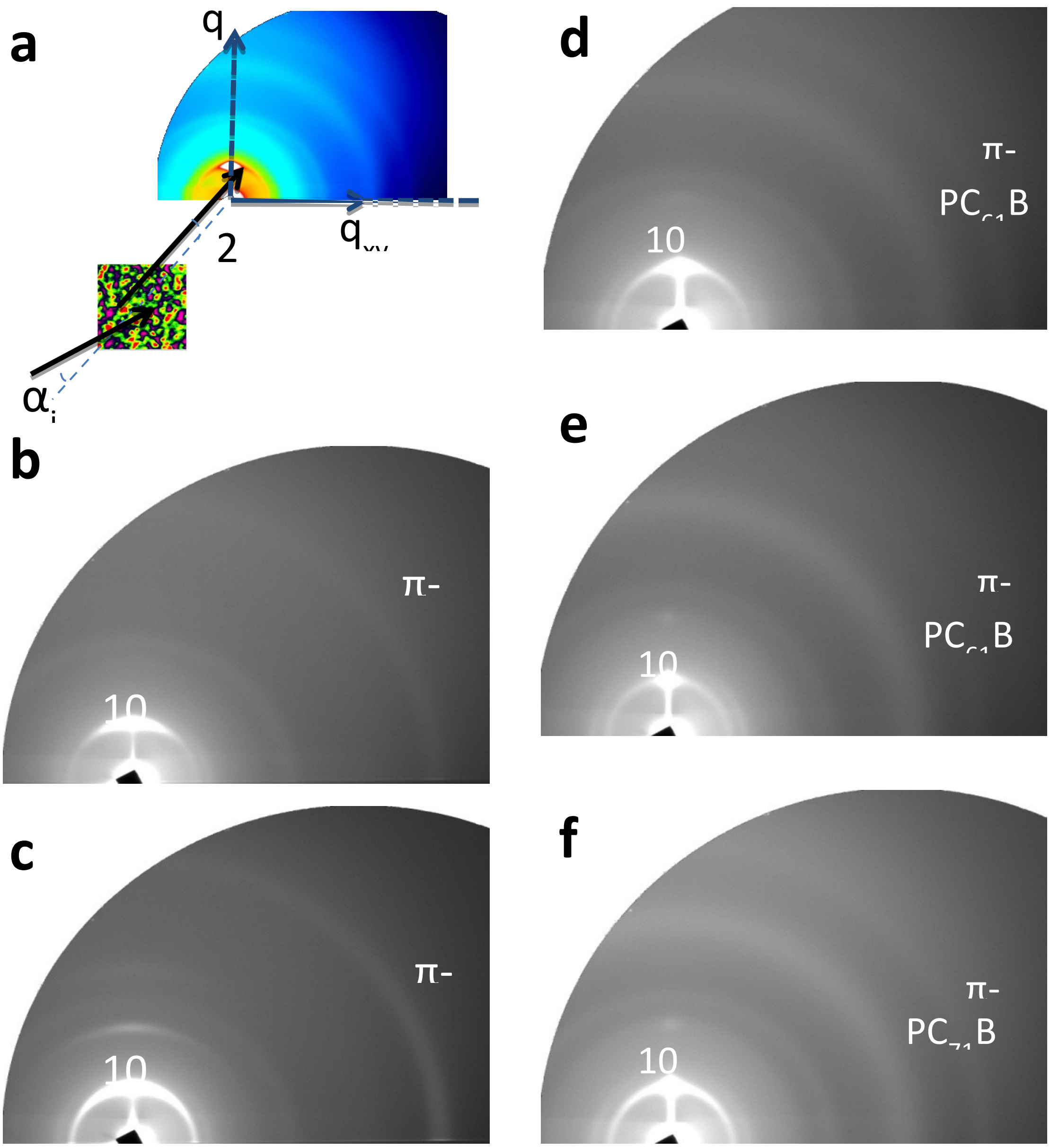

Fig. S4 a) Scheme of the GIWAXS diffraction geometry, where q_z and q_{xy} are directions in the detector reference frame. The absolute value of the scattering vector, q, is determined from the total scattering angle 2θ, $q = 4\pi\sin 2\theta / \lambda$. b) and c) show 2D diffraction patterns of the pristine films for **1** and **2**, respectively. The (100) Bragg peak appears at q = 0.392 $Å^{-1}$ for 1 and at q = 0.370 $Å^{-1}$ for 2 (see Table 2). Although edge-on is the predominant orientation (parallel orientation of the (100) planes on the surface), the arching of the intensity around (100) indicates a certain angular distribution of the orientation of the oligomer crystallites. For both films the scattering ring corresponding to the π-π stacking of the oligomers is present (q = 1.80 $Å^{-1}$) with associated spacing of ≈ 3.5 Å. On the right, 2D diffraction patterns of the blends after SVA: d) **1**:$PC_{61}BM$, e) **2**:$PC_{61}BM$, and f) **2**:$PC_{71}BM$.

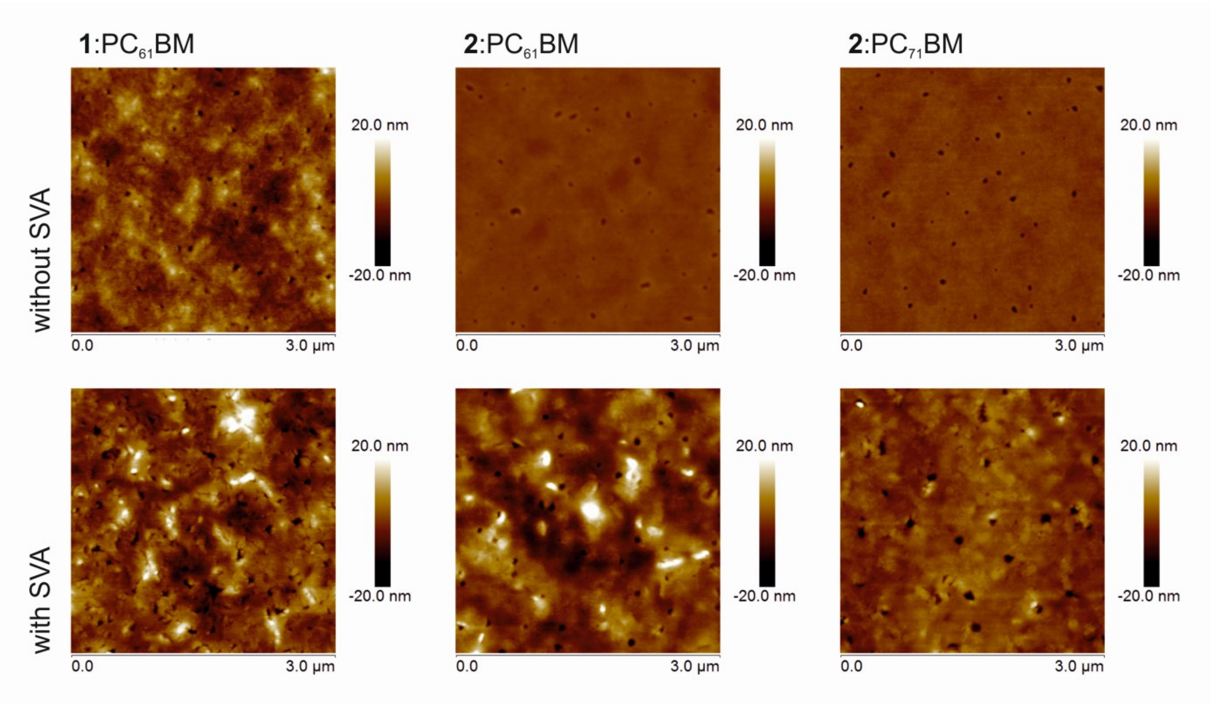

Fig. S5 AFM topography images of **1**:$PC_{61}BM$, **2**:$PC_{61}BM$ and **2**:$PC_{71}BM$ films with and without SVA.

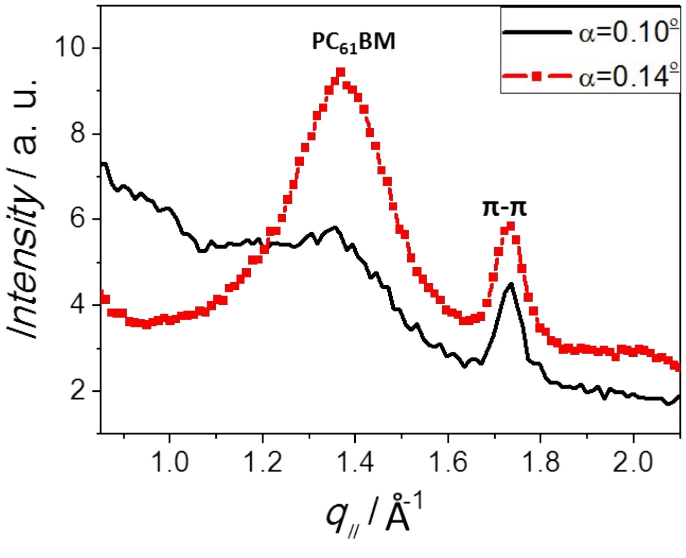

Fig. S6 In-plane scans for the solvent-vapor annealed **2**:$PC_{61}BM$ films collected with a point detector for incident angle of 0.10° (below the critical angle, i. e. penetration depth limited to few nanometers) and 0.14° (above the critical angle, i. e. penetration of the x-rays in the bulk of the film).

In order to resolve peaks with better signal/noise ratio, GIWAXS employing a point-detector was performed. The in-plane scans are shown in the Fig. S5, showing the peaks corresponding to the PCBM and the π-π stacking of the oligomers for two incident angles of 0.10º and 0.14º. At incidence angle of $0.10 < \alpha_c$ (penetration depth ~ 7 nm), the intensity of the oligomers in relation to PCBM is significantly larger than for the incident angles $>\alpha_c$, for which the penetration depth exceeds 60 nm. This gives evidence of oligomer enrichment at the top surface of the film.

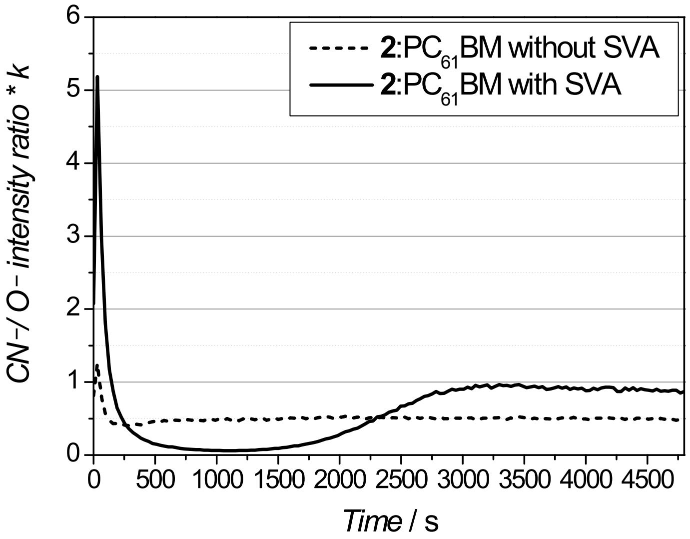

Fig. S7 Ratio of CN26⁻ to O16⁻ * k of the SIMS measurement of **2**:$PC_{61}BM$ films without (dash) and with (solid) SVA.

In order to calculate the ratio of oligomer **2** to $PC_{61}BM$ in the SIMS depth profile only the section of the absorber layer was regarded. The signals of CN26⁻ and O16⁻ were summed (in the range of 0 s to 4800 s) and the sums were divided by each other and multiplied by a factor k (Fig. S6) to get a ratio of 1:2 within the whole absorber layer (which is the ratio of oligomer **2** and $PC_{61}BM$ in the used absorber solution). The factor k is necessary to take into account the different portion of CN^- and O^- in the molecule **2** and $PC_{61}BM$, respectively, as well as the different ionization probabilities of CN^- and O^- in the negative SIMS signals.

Table S1 R_s and R_p values for solar cells of **1:**$PC_{61}BM$, **2:**$PC_{61}BM$ and **2:**$PC_{71}BM$.

	SVA (s)	**PCE (%)**	***R$_s$*** **(Ohm/cm^2)**	***R$_p$*** **(Ohm/cm^2)**
1:$PC_{61}BM$ (1:2)$^{a)}$	0	3.8	5.61	944
	120	4.6	3.20	1180
2:$PC_{61}BM$ (1:2)$^{a)}$	0	1.1	4.41	285
	90	6.1	2.25	1744
2:$PC_{71}BM$ (1:2)$^{b)}$	0	1.1	3.19	247
	90	7.1	1.97	1670

$^{a)}$solution casted at 50°C, $^{b)}$solution casted at room temperature.

As it can be seen in Table S1, SVA improves the values of both R_s and R_p: The series resistance is reduced for solar cells with oligomer **1** and **2** accompanied by an increase of the parallel resistance.
Noticeable, for cells with oligomer **2** the change in R_p is much bigger (more than factor 6) than for cells with oligomer **1**, due to the fact that oligomer **1** delivers even without SVA relative good solar cells.
It has to be noticed that fitting of the IV curves was difficult, as the curves are not ideal and give diode factors >2. Therefore the given values should only demonstrate the trend of changes upon SVA.